

S4Sleep: Elucidating the design space of deep-learning-based sleep stage classification models

Tiezhi Wang and Nils Strodthoff

Abstract—Scoring sleep stages in polysomnography recordings is a time-consuming task plagued by significant inter-rater variability. Therefore, it stands to benefit from the application of machine learning algorithms. While many algorithms have been proposed for this purpose, certain critical architectural decisions have not received systematic exploration. In this study, we meticulously investigate these design choices within the broad category of encoder-predictor architectures. We identify robust architectures applicable to both time series and spectrogram input representations. These architectures incorporate structured state space models as integral components, leading to statistically significant advancements in performance on the extensive SHHS dataset. These improvements are assessed through both statistical and systematic error estimations. We anticipate that the architectural insights gained from this study will not only prove valuable for future research in sleep staging but also hold relevance for other time series annotation tasks.

Index Terms—Decision support systems, Electroencephalography, Machine learning algorithms, Time series analysis

I. INTRODUCTION

SLEEP disorders, which are prevalent and can have severe implications for patients’ health and overall well-being, are known to lead to significant morbidity [1], [2]. Primary care practice commonly involves managing various significant sleep disorders including insomnia, sleep-disordered breathing, hypersomnia/narcolepsy, circadian rhythm disorders, parasomnias, and sleep-related movement disorders [2]. Within clinical practice, sleep staging is necessary to understand the structure and quality of sleep, enabling the diagnosis of sleep disorders and informing appropriate treatment strategies. It also facilitates sleep research, providing insights into sleep patterns and physiological processes during different stages of sleep.

Sleep staging Sleep staging refers to inferring the state of human sleep into one of five or six sleep stages (wake(W), non-rapid-eye-movement (N1-N3 or N1-N4 depending on annotation standard), rapid-eye-movement (REM)). The gold standard measurement setup for sleep staging is polysomnography (PSG), which typically comprises a range of different sensor modalities such as electroencephalography (EEG), electrooculogram (EOG), electromyography (EMG), electrocardiography (ECG), pulse oximetry, and respiratory signals. The EEG represents the most important modality, which is why most single-channel automatic sleep staging algorithms rely on a single

(average) EEG channel. EEG montages and the availability and details of the availability of other sensor modalities vary widely across datasets. The annotation process is formalized through AASM guidelines [3] or R&K guidelines [4], and is usually performed for segments of 30s, referred to as epochs. The assessment of an overnight PSG recording by a human expert is a tedious process, which requires up to several hours of work, and is subject to a high inter-rater variability [5], [6]. This is why automatic sleep scoring systems consistent with human level performance within inter-rater variability could represent an enormous improvement for the sleep stage assessment. While the field of automatic sleep staging by means of machine learning has evolved a lot recently, compelling evidence on several important design decisions is lacking.

Design choices Machine learning and in particular deep learning algorithms have improved tremendously in the past few years. In the field of sleep staging, such algorithms have developed into a maturity where the performance is on par with the best human raters. The predominantly used architectures, apart from the U-sleep model [7], which relies on a U-net architecture, are sequence-to-sequence models typically with a local CNN model (operating on time-domain input, frequency-domain input or, most recently, combinations of both [8]) as encoder extractor and commonly a Long Short Term Memory (LSTM) model or most recently also transformer [9] models to aggregate the features according to the temporal context [10]. We put the different design choices to a thorough test. In particular, we explore structured state space sequence (S4) models, which are well-known for their ability to capture long-range dependencies in time series data [11] and have been successfully applied to other physiological time series data, such as electrocardiography data [12].

Contributions We systematically investigate design choices for long time series annotation tasks at the particular example of sleep staging. Here, we summarize the core contributions of this work:

- 1) *Model architecture: encoder* Through a thorough analysis of short-range single-epoch input models, we identify optimal encoder architectures that utilize structured state space models for both time series and spectrogram inputs. When extending the input size to multiple epochs, these same encoders yield optimal performance.
- 2) *Model architecture: predictor* Alongside the identified encoders, we systematically determine the most suitable predictor models for combining information across multiple input epochs. For time series input, structured state

space models are optimal, while transformer models perform best for spectrogram input.

- 3) *Insights from optimal model* With the optimal models identified, we offer comparative insights into different input representations and the number of input channels. This analysis includes both statistical and systematic error estimates. In particular, the identified S4Sleep models yield statistically significant performance improvements on the large-scale SHHS dataset.

II. METHODS

A. Models

Encoder-Predictor Model We follow the design choice of encoder-predictor models as the predominantly used approach in the literature. It is also preferable on general grounds as it implements the principle of scale separation [13] and hierarchical representations [14], [15]. Roughly speaking, the raw input (either raw time series or spectrograms) is processed by an encoder model, which typically returns a semantically enriched, temporally downsampled representation. The conventional approach in the field is to reduce the temporal resolution to a single token per sleep staging epoch but it is also possible to chose a temporally more finegrained resolution for the intermediate representation. Consequently, this representation is passed to the predictor model, which integrates the information across tokens on the epoch or sub-epoch-level. Typical predictor models leave the temporal resolution of the input signal unchanged. Finally, the output of the predictor model is processed by a prediction head to produce epoch-level predictions. In the case of an epoch-level encoder, this can be as simple as a MLP or a single linear layer shared across all output tokens. In the case of a sub-epoch-level encoder, it will typically be preceded by a local pooling layer to reach an output representation that matches the required temporal resolution at epoch-level. We summarize the encoder-predictor models schematically in Fig. 1. Different encoder and predictor architectures can be mixed in a modular fashion and one of the core contributions of this work is to provide a structured assessment of their different components and their interplay. Below, we describe considered encoder and predictor architectures in detail. For additional details, we refer to the accompanying code repository [16].

1) *Encoder architectures: Single-epoch encoder* For a single-epoch time series input, we utilized an encoder architecture that comprises two one-dimensional convolutional layers. Each layer consists of 128 features, a kernel size of 3, a stride of 2, corresponding to a moderate downsampling factor of 4, interleaved by ReLU activation functions. In the case of spectrogram input, we reshape the input to join frequency and channel dimensions, which subsequently allows to a further processing using one-dimensional convolutions. In this case, we employed a similar encoder structure with two 1D convolutional layers. Here, we use 128 features, a kernel size of 3 and a stride of 1 interleaved by GeLU activation functions. This particular choice was inspired by the encoder used in state-of-the-art speech recognition models operating on spectrograms as input data [17] and reduces to the former in

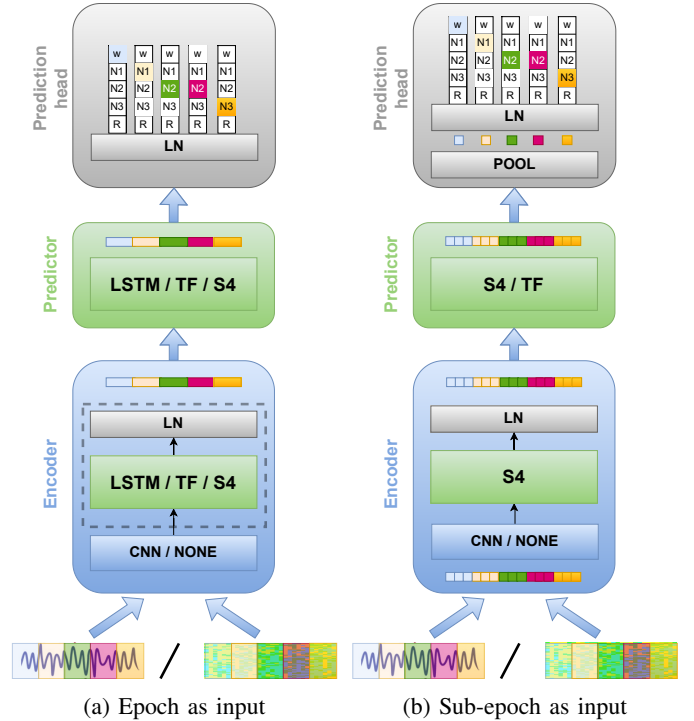


Fig. 1: Schematic representation of the encoder-predictor model architectures used in this work: (left) Widely used architecture with (epoch) encoder. The parts within the dashed box are components of the epoch encoder designed for processing multi-epoch input, where input tokens of the predictor align with the number of epochs predicted simultaneously. (right) Model with epoch encoder operating on a sub-epoch level, where the predictor works at a temporally higher resolution compared to the single-epoch case and local pooling aligns the number of output tokens with the number of input epochs again.

the case of a single input channel. To simplify the notation, we refer to both encoders as *CNN* encoder but refer with it to the respective convolutional encoders for time series/spectrogram data.

No encoder We also conducted experiments with architectures without explicit encoders (*NONE*), where the input is passed directly to the respective predictor models. In the case of time series input, the input sequence is just processed through a linear layer mapping from the number of input channels to the appropriate model dimension of the predictor model. In the case of spectrogram input, we first reshape channel and frequency axes into a common axis and then proceed with a linear layer as in the case of time series input.

Epoch encoder For multi-epoch time series inputs, we consider two different strategies: The first option is to use an entire single-epoch model as encoder. These are then by themselves composed of encoder, predictor and prediction head. We refer to such encoders as *epoch encoders*. For the encoders within such models we use the convolutional encoders for time series/spectrogram input described above and the prediction head is a global average pooling layer (or a local average pooling layer in the case of sub-epoch encoders). We

distinguish different epoch encoders based on the respective predictor model they use, see also the detailed discussion of the predictor model architectures below. We consider three different architectures: A two-layer, bidirectional LSTM model [18], a four-layer transformer model [19], or a four-layer S4 model. To ensure that the total number of trainable parameters and hence the model complexity approximately remains within a same magnitude, we set the model dimensions to 512, 256, and 512 for LSTM, transformers, and S4, respectively. The dropout rates stand at 0.1 for the transformer models and 0.2 for the S4 models. Each transformer layer features 8 heads, while the state dimension of S4 is set to 64. We refer to the corresponding epoch encoders as *EELSTM*, *EETF*, and *EES4*. As a special case, we also consider an epoch encoder with a S4 model as predictor but without explicit encoder (*NONE*), as described in the previous paragraph, and refer to it to as *EENS4*.

Strided CNN The second option to reach a heavily temporally downsampled intermediate representation that is appropriate for further processing is through the use of strided convolutions. This approach is inspired by encoders used in speech recognition models operating on raw waveform data such as *wave2vec* [20]. Here, we use four 1D convolutional layers each with feature sizes 512, kernel sizes of 9-9-3-3, and stride sizes of 5-5-2-2, resulting in a temporal downsampling factor of 100, interleaved with ReLU activations. We refer to this encoder as *SCNN* (for strided CNN) encoder. For multi-epoch spectrogram input, we have the option to utilize the CNN encoder (*CNN*) described in the paragraph on single-epoch encoder. In this case there is no need for a strong temporal downsampling as the spectrograms by themselves already come at a 100 times smaller temporal resolution compared to the original time series input. In this sense, the simple CNN encoder for spectrograms can be regarded as analogue of the strided CNN encoder for raw time series.

2) *Predictor architectures*: We consider the same three architectures for the predictor model as previously introduced in the context of epoch encoders with similar hyperparameter choices, i.e. a two-layer LSTM model (*LSTM*), four-layer transformer (*TF*) and four-layer S4 model (*S4*).

3) *Prediction head architectures*: The prediction head architecture is just comprised of a single linear layer. Only in the case of sub-epoch encoder and no encoder (*NONE*), it is preceded by a local average pooling layer with appropriate kernel size to reduce the temporal resolution of the output to one output token per epoch.

B. Datasets

Sleep-EDF (SEDF) The SEDF database comprises 197 sleep recordings from both healthy subjects (subset SC, 153 recordings) and from patients experiencing mild difficulty falling asleep (subset ST, 44 recordings) [21], [22]. All recordings include EOG, Fpz-Cz, and Pz-Oz EEG channels, sampled at 100 Hz. The recordings are manually scored into W, N1-N4, REM, MOVEMENT and UNKNOWN according to the R&K guidelines. Following the common preprocessing in the literature, we merged N3 and N4 (into N3), and excluded

TABLE I: Summary of datasets

Dataset	Recordings	Included channels
Sleep EDF [21], [22]	197	EEG (Fpz-Cz, Pz-Oz), EOG (horizontal)
SHHS Visit 1 [23], [24]	5463	EEG (C3-A2, C4-A1), EOG (left, right), EMG

data segments labeled as MOVEMENT and UNKNOWN. We conducted experiments on multi-channel data containing two EEG channels (Fpz-Cz and Pz-Oz) and one EOG channel (horizontal), as well as on single-channel data consisting only of the Fpz-Cz EEG channel. We performed a random split of the recordings, allocating 80% of the recordings for training, 10% for validation and 10% for testing. We release these splits for later reproducibility [16].

SHHS The Sleep Heart Health Study (SHHS) dataset includes polysomnography data collected from participants across two overnight visits (Visit 1 and Visit 2), with several intervening years for follow-up [23], [24]. For our study, we utilized data from SHHS Visit 1, which includes two EEG channels, two EOG channels, and one EMG channel, among other signals. The recordings are manually scored according to the R&K guidelines. For comparability with literature approaches [25], recordings that did not contain all stages W, N1-N4, and REM sleep stages were excluded. This resulted in the retention of 5463 recordings. As with SEDF, we merged N3 and N4, and excluded data segments labeled as MOVEMENT and UNKNOWN. The dataset was resampled to 100 Hz. We conducted experiments on multi-channel data containing two EEG channels (C4-A1 and C3-A2), two EOG channels (left and right), and one EMG channel, as well as on single-channel data consisting only of the C4-A1 EEG channel. We performed a random split of the recordings, allocating 70% of the recordings for training and 30% for testing. Additionally, we set aside 100 recordings from the training set specifically for validation purposes. Again, we release these splits for later reproducibility as part of the accompanying code repository [16].

Preprocessing Both datasets were used in terms of two different input representations, raw time series and spectrograms. Spectrograms were generated in a manner consistent with L-SeqSleepNet [25]. Each channel signal from a 30-second epoch was transformed to generate a log-magnitude time-frequency image. This involved dividing the signal into 29 time steps and 129 frequency bins using the short-time Fourier transform (STFT) with a window length of 2 seconds and a 1 second overlap. A Hamming window and a 256-point fast Fourier transform (FFT) were used in the process. The resulting amplitude spectrum for each channel underwent logarithmic transformation, creating a time-frequency image. The raw time series input underwent no further preprocessing.

C. Training procedure and performance evaluation

Training To mitigate issues due to imbalanced label distributions that are typical for this task, we use focal loss [26] as loss function. For all experiments, we use a fixed effective batch size of 64 achieved through gradient accumulation. We

performed experiments with learning rates determined via the learning rate finder [27] as well as with a fixed learning rate of 0.001 for each experiment. The learning rate yielding superior validation set performance was selected. We train models using a constant learning rate using AdamW [28] as optimizer. For training and validation, we divide the whole input sequence of a given sample into consecutive segments whose lengths coincide with the model’s input size. For SEDF, the models underwent training for 50 epochs, with validation performed after each training epoch. For SSHS, we found longer training beneficial (in terms of training iterations) and train for 30 epochs. For the final test set evaluation, we select the model at the training epoch with the best validation set performance (in terms of macro F1 score). We train on non-overlapping crops of the specified input size. During test time, we split the input sequences into segments of the same length but use a smaller stride length coinciding with the length of a single epoch. For most segments, we obtain in this way multiple predictions corresponding to different positions in the input sequence passed to the model. We subsequently average all available predictions on the level of output probabilities for a given segment.

Performance evaluation Irrespective of the input size the procedure described in the previous section yields a probabilistic model prediction per test/validation set epoch. We can then compare dichotomized model predictions with the ground truth. The most commonly used metric in the field is the macro- F_1 -score computed as the mean of the individual label F_1 -scores. Due to its widespread use, we mostly focus on F_1 -score to compare model performance, but also indicate the individual label scores, as well as the accuracy and the macro-average of the area under the receiver operating curve (AUC), as the only non-thresholded metric among the considered metrics. Even though accuracy is commonly used in the field, it is worth stressing that the results is strongly affected by label imbalance, which means in this case that the score is biased towards the majority classes N2 followed by W.

III. RESULTS

A. Model selection on SEDF

We proceed in two steps: To limit the search space, we start by considering models that take a single epoch as input. Based on the insights of this experiment, we proceed to multi-epoch models and fix further design choices there to identify the best-suited model architecture for sleep staging. After training, we perform model selection and pick the model from the training epoch with the largest SEDF validation set score (macro F_1). We only report validation set performances at this point to avoid overfitting to the SEDF test set. We acknowledge the fact that the use of the validation set both for model selection and score estimation will lead to a slight overestimation of the generalization performance of the model. However, we stress that we are only interested in a comparative assessment at this stage. A proper hold-out set evaluation on unseen test data will be deferred to Section III-B.

Nevertheless, an uncertainty estimate for the achieved results is very desirable already at this stage to assess the

significance of the performance differences. There are two main sources of uncertainty that are of main interest here: the uncertainty in the final score due to the randomness of the training process and the uncertainty due to the finiteness and particular composition of the test/validation set. The former uncertainty is typically assessed through multiple training runs. For computational reasons, we resort to a single training run at this stage and defer a proper assessment to the evaluation in Section III-B. However, we can assess the second kind of uncertainty through (empirical) bootstrapping ($n = 1000$ iterations) on the test set. To determine if the difference in performance (according to macro-F1 score as metric) is significant, we calculate 95% confidence intervals for the score difference. If the confidence interval for the performance difference does not overlap with zero, we regard the performances of the two models as statistically significantly different.

Single-epoch prediction models For single epoch models, we assess the impact of the predictor model ($S4$, TF , $LSTM$). For both input representations, we consider both a convolutional encoders (CNN) as well as no encoder ($NONE$). The results for raw time series as input both for single- as well as multi-channel clearly distinguish $CNN+S4$ as best-performing architecture. For time series input, a CNN encoder turns out to be beneficial as compared to using no encoder. On the contrary, for spectrogram data, the using no encoder turns out to be the more favorable choice. These results suggest that the architectural choices are inherently tied to the input representations. The difference between both encoder choices for identical predictor model is most strongly pronounced for $S4$ as predictor, whereas TF is barely influenced by this choice. The best-performing model on spectrogram input according macro- F_1 score turns out to be $NONE+S4$, again across both channel settings. Looking at overall best performance, raw-time-series-based models are outperformed by spectrogram-based models for multi-channel input while the opposite ordering is observed in the single-channel case. In line with expectations, multi-channel input seems to exhibit a systematic positive effect compared to single-channel input. We use these insights from the single-epoch case to construct multi-epoch prediction models using the identified encoder-predictor combinations as epoch encoders.

Multi-epoch prediction models: time series input For raw time series, we consider the best-performing encoder-predictor combination ($CNN+S4$) from the previous sections as epoch encoder ($EES4$) in combination with the three different predictor architectures ($S4$, TF and $LSTM$) introduced above. In addition, we investigate a strided convolutional encoder ($SCNN$) again in combination with the three different predictor architectures. Finally, we also consider the case of matching epoch encoder and predictor architectures ($EETF+TF$ and $EELSTM+LSTM$). We summarize the results of our experiments for 15 epochs input in Table III. Whereas $S4$ and TF show a comparable performance in combination with the $SCNN$ encoder, $EES4+S4$ is clearly singled out (with a rather large gap to the second-best combination $SCNN+TF$) as best-performing architecture in the case of the $EES4$ encoder both in the single- and in the multi-channel setting. Comparing

TABLE II: Comparing different encoder and predictor architectures for a *single epoch input size* trained on SEDF based on validation set scores. Best results for a given channel configuration are marked in bold face.

channels	features	encoder	predictor	F_1 (\uparrow)							acc. (\uparrow)	macro AUC (\uparrow)
				macro	W	N1	N2	N3	REM			
EEG \times 2, EOG \times 1	raw	CNN	S4	0.780	0.916	0.489	0.851	0.822	0.824	0.823	0.961	
		CNN	TF	0.745	0.913	0.439	0.811	0.802	0.760	0.793	0.950	
		CNN	LSTM	0.767	0.917	0.482	0.840	0.807	0.787	0.813	0.957	
		NONE	S4	0.776	0.910	0.510	0.837	0.802	0.821	0.813	0.960	
		NONE	LSTM	0.729	0.903	0.412	0.810	0.792	0.728	0.778	0.942	
		CNN	S4	0.750	0.914	0.433	0.830	0.773	0.802	0.808	0.951	
	spec	CNN	TF	0.775	0.911	0.488	0.844	0.798	0.833	0.817	0.956	
		CNN	LSTM	0.771	0.920	0.453	0.842	0.806	0.836	0.821	0.955	
		NONE	S4	0.783	0.915	0.510	0.851	0.802	0.836	0.822	0.960	
		NONE	TF	0.777	0.915	0.494	0.850	0.799	0.827	0.822	0.961	
		NONE	LSTM	0.775	0.913	0.479	0.846	0.813	0.825	0.820	0.959	
		CNN	S4	0.749	0.908	0.421	0.841	0.811	0.762	0.803	0.954	
EEG \times 1	raw	CNN	TF	0.710	0.880	0.355	0.822	0.818	0.675	0.770	0.954	
		CNN	LSTM	0.744	0.902	0.403	0.852	0.821	0.744	0.802	0.951	
		NONE	S4	0.743	0.897	0.454	0.829	0.799	0.734	0.786	0.947	
		NONE	LSTM	0.714	0.887	0.396	0.831	0.801	0.653	0.770	0.938	
		CNN	S4	0.695	0.855	0.400	0.810	0.766	0.646	0.744	0.931	
	spec	CNN	TF	0.723	0.882	0.386	0.836	0.784	0.726	0.782	0.942	
		CNN	LSTM	0.730	0.882	0.410	0.832	0.797	0.728	0.785	0.944	
		NONE	S4	0.734	0.884	0.417	0.831	0.796	0.742	0.787	0.949	
		NONE	TF	0.721	0.873	0.415	0.830	0.785	0.701	0.769	0.942	
		NONE	LSTM	0.715	0.867	0.362	0.832	0.798	0.717	0.775	0.937	

different encoders for fixed predictor model, the *EES4* encoder clearly shows the strongest performance confirming the results from the single-epoch experiments from above.

Multi-epoch prediction models: spectrogram input As in the case of raw time series input, we consider an epoch encoder built from the best-performing encoder-predictor combination (*NONE+S4*) identified in the single-epoch experiment *EENS4*. As the spectrogram input is already heavily downsampled by a factor of 100 along the temporal direction compared to the original input resolution of the raw time series, there is no need for excessive downsampling or the use of epoch encoders. Therefore, we also explore the use of a conventional CNN encoder (*CNN*) and the use of no encoder (*NONE*), i.e., architectures identical to the single-epoch case. We combine each of these encoders with three predictors resulting in overall nine encoder-predictor combinations for each of the two channel configurations. It is worth stressing that the use of spectrogram input with epoch encoders corresponds to the most commonly used design choices in the field, for example *EELSTM+LSTM* can be roughly identified with the architecture used in [10]. As before, we summarize the results of our experiments for 15 epochs input in Table III. Both in the single-channel as well as in the multi-channel case, the epoch encoder *EES4* is clearly singled out as best-performing encoder architecture. Even though the input length of the predictor model is in the case of epoch encoders identical to that of the corresponding predictor in the raw time series case, the *S4* does not turn out as strong as in the raw time series case. Interestingly, in the multi-channel case the three architectures *EENS4+TF*, *EENS4+LSTM* and *NONE+S4*, i.e. an architecture without epoch encoder, yield similar performance, the single-channel setting is clearly dominated by *EENS4+TF*.

Multi-epoch prediction models: comparative assessment For time series as input, the *EES4* encoder represents the

key component to achieve competitive performance, overall *EES4+S4* turns out as best-performing combination. For spectrograms as input, as we are interested in identifying architectures that can generalize also to other datasets and channel configurations, we identify *EENS4+TF* (as opposed to *NONE+S4*) as architecture of choice for models operating on spectrograms as input data. It is worth noting the consistent performance gaps between the best-performing models operating on time series compared to those operating on spectrograms (0.820 vs. 0.815 for multi-channel and 0.801 vs. 0.797 for single-channel). As in the case of a single input channel, we find a consistent improvement of multi-channel models over single-channel models.

Full-epoch vs. sub-epoch encoder In addition to the encoders for single or multiple epochs as input, we also conducted experiments with sub-epoch-level encoders. We used $1/n$ of an epoch as input unit, which corresponds to n output tokens per input epoch after the encoder, and consider values for n of 2, 5, and 10 for the overall best-performing model architecture (*EES4+S4*). Notation-wise, we refer to a sub-epoch encoder with $n = 5$ as *1/5 EES4*, for the case of a *S4* epoch encoder. The results shown in Table IV suggest that the choice of sub-epoch level can influence the model performance. In the case of single-channel input, $n = 5$ exhibited superior performance in terms of macro F1 scores compared to the single-epoch encoder ($n = 1$). Even though the model performance is on par with the standard epoch encoder in the case of multi-channel input, we strive to identify architectures that work reliably across different situations and we therefore still select a sub-epoch encoder ($n = 5$) for our final experiments. In the case of spectrogram input, the multi-channel case favors both $n = 1$ and $n = 5$ but the single-channel case clearly distinguishes $n = 1$. As we are looking for an architecture that generalizes across channel configurations, we use the conventional epoch

TABLE III: Comparing different encoder and predictor architectures for 15 epochs input size trained on SEDF based on validation set scores. The scores marked with an asterisk (*) represent models whose scores do not exhibit statistically significant differences (according to macro-F1 score) compared to the best-performing model of the respective channel and input-modality combination. The remaining notation follows Tab. II.

channels	features	encoder	predictor	F_1 (\uparrow)						acc. (\uparrow)	macro AUC (\uparrow)
				macro	W	N1	N2	N3	REM		
EEG \times 2, EOG \times 1	raw	EES4	S4	0.820	0.931	0.612	0.862	0.798	0.895	0.851	0.973
		EES4	TF	0.812	0.931	0.563	0.864	0.815	0.888	0.851	0.972
		EES4	LSTM	0.803	0.925	0.538	0.862	0.818	0.871	0.843	0.969
		SCNN	S4	0.787	0.919	0.515	0.840	0.809	0.854	0.830	0.964
		SCNN	TF	0.804	0.922	0.546	0.865	0.817	0.872	0.844	0.969
		SCNN	LSTM	0.795	0.922	0.537	0.860	0.786	0.870	0.840	0.968
		EETF	TF	0.783	0.913	0.480	0.849	0.805	0.866	0.830	0.963
		EELSTM	LSTM	0.795	0.922	0.523	0.854	0.812	0.861	0.837	0.967
	spec	EENS4	S4	0.811	0.928	0.556	0.867	0.818	0.886	0.851	0.970
		EENS4	TF	0.815*	0.928	0.578	0.857	0.827	0.884	0.846	0.970
		EENS4	LSTM	0.815*	0.931	0.563	0.865	0.824	0.892	0.853	0.969
		CNN	S4	0.788	0.913	0.542	0.848	0.774	0.864	0.829	0.963
		CNN	TF	0.788	0.909	0.506	0.854	0.801	0.872	0.832	0.966
		CNN	LSTM	0.799	0.924	0.545	0.862	0.789	0.876	0.844	0.968
		NONE	S4	0.815*	0.930	0.558	0.863	0.823	0.898	0.853	0.969
		NONE	TF	0.782	0.913	0.479	0.847	0.808	0.864	0.828	0.961
EEG \times 1	raw	EES4	S4	0.801	0.913	0.569	0.868	0.801	0.853	0.839	0.970
		EES4	TF	0.763	0.905	0.472	0.845	0.813	0.781	0.813	0.961
		EES4	LSTM	0.770	0.911	0.480	0.853	0.815	0.790	0.822	0.963
		SCNN	S4	0.786	0.909	0.504	0.857	0.819	0.841	0.833	0.965
		SCNN	TF	0.789	0.916	0.497	0.867	0.813	0.851	0.840	0.967
		SCNN	LSTM	0.781	0.916	0.506	0.866	0.757	0.869	0.834	0.966
		EETF	TF	0.732	0.899	0.413	0.831	0.789	0.725	0.792	0.947
		EELSTM	LSTM	0.783	0.908	0.496	0.870	0.814	0.828	0.834	0.964
	spec	EENS4	S4	0.784	0.897	0.530	0.866	0.784	0.842	0.827	0.962
		EENS4	TF	0.797	0.911	0.536	0.865	0.812	0.861	0.839	0.968
		EENS4	LSTM	0.790	0.904	0.549	0.858	0.798	0.843	0.832	0.965
		NONE	S4	0.777	0.891	0.501	0.861	0.803	0.828	0.824	0.962
		NONE	TF	0.741	0.876	0.438	0.840	0.783	0.767	0.789	0.950
		NONE	LSTM	0.739	0.874	0.441	0.839	0.767	0.773	0.791	0.945
		CNN	S4	0.764	0.889	0.472	0.848	0.787	0.821	0.810	0.956
		CNN	TF	0.779	0.898	0.481	0.859	0.808	0.847	0.828	0.960
CNN	LSTM	0.780	0.905	0.491	0.859	0.798	0.846	0.827	0.963		

encoder ($n = 1$) in this case.

Summary At this point we recapitulate the findings of the experiments presented in the previous paragraphs: For time series input, we identify $1/5$ EES4+S4, i.e., an epoch encoder leveraging a S4 model operating on a sub-epoch level of $1/5$ of an epoch combined with another S4 model as predictor, as best-performing architecture and refer to it as $S4Sleep(TS)$. For spectrogram input, we identify EENS4+TF, i.e., again an epoch encoder leveraging an S4-model internally but this time operating on the input directly, as best-performing architecture and call it $S4Sleep(Spec)$.

B. Performance evaluation

Training procedures In this section, we put the identified architectures $S4Sleep(TS)$ and $S4Sleep(Spec)$ to a test. First, we evaluate the identified optimal model architectures for multi-channel and single-channel input on the SEDF test set. As the whole analysis so far concentrated on SEDF, we aim to demonstrate that the identified architectures also generalize to other (large-scale) datasets after retraining. To this end, we trained and evaluated the same model architectures with identical hyperparameters (except for the learning rate, which

was determined using the learning rate finder as described above).

Score estimation We refrain from using crossvalidation, which is a popular score estimation scheme in the literature, in particular on SEDF, but rather use a simple holdout set evaluation both for SEDF and SHHS. First, reliable statistical error estimates for crossvalidation are still an unresolved problem [29]. However, we see statistical uncertainties as essential components to assess the statistical significance of our findings. We allocated 80% of the SEDF for training the model, maintaining a consistent number of recordings for each training iteration as used for example in the 5-fold validation conducted on the full SEDF dataset in [30]. We therefore believe that even though our results were achieved through a different kind of score estimation, that our hold-out evaluation scores with statistical uncertainties are comparable to cross-validation results from the literature. For full transparency, we indicate the precise dataset choice as well as score estimation method in the for all considered methods in the final results in Tab. V.

Uncertainty and statistical significance To assess the systematic uncertainty due to the randomness of the training process, we perform three separate training runs for each scenario and

TABLE IV: Comparing epoch encoder and sub-epoch encoder on SEDF based on validation set scores. Notation as in Tab. III.

channels	features	fraction	encoder	predictor	F_1 (\uparrow)						acc. (\uparrow)	macro AUC (\uparrow)
					macro	W	N1	N2	N3	REM		
EEG \times 2, EOG \times 1	raw	1	EES4	S4	0.820*	0.931	0.612	0.862	0.798	0.895	0.851	0.973
		1/2	EES4	S4	0.814*	0.939	0.586	0.875	0.774	0.897	0.861	0.974
		1/5	EES4	S4	0.820*	0.936	0.598	0.859	0.819	0.890	0.853	0.972
		1/10	EES4	S4	0.814	0.929	0.574	0.865	0.815	0.886	0.850	0.972
	spec	1	EENS4	TF	0.815*	0.928	0.578	0.857	0.827	0.884	0.846	0.970
		1/2	EENS4	TF	0.818*	0.930	0.582	0.861	0.822	0.894	0.851	0.971
		1/5	EENS4	TF	0.800	0.906	0.557	0.854	0.803	0.883	0.832	0.967
		1/10	EENS4	TF	0.801	0.919	0.554	0.860	0.788	0.885	0.842	0.966
EEG \times 1	raw	1	EES4	S4	0.801*	0.913	0.569	0.868	0.801	0.853	0.839	0.970
		1/2	EES4	S4	0.802*	0.923	0.559	0.868	0.806	0.854	0.844	0.969
		1/5	EES4	S4	0.804*	0.920	0.559	0.852	0.817	0.873	0.837	0.968
		1/10	EES4	S4	0.784	0.912	0.482	0.862	0.820	0.845	0.834	0.962
	spec	1	EENS4	TF	0.797*	0.911	0.536	0.865	0.812	0.861	0.839	0.968
		1/2	EENS4	TF	0.787	0.895	0.530	0.860	0.801	0.848	0.827	0.961
		1/5	EENS4	TF	0.785	0.913	0.511	0.858	0.787	0.856	0.832	0.965
		1/10	EENS4	TF	0.785	0.909	0.509	0.858	0.803	0.845	0.831	0.961

report the median F_1 -score along with the interquartile ranges as fluctuation measure. We estimate the statistical uncertainty due to the finiteness and composition of the test set through empirical bootstrapping ($n = 1000$ iterations) on the test set. We report the median of the three bootstrap uncertainty measures across the three training runs. We report the final results in the form (median macro $- F_1$) \pm (systematic uncertainty) \pm (statistical uncertainty).

To assess the statistical significance of performance differences while also incorporating the uncertainty due to the randomness of the training process, we follow the methodology proposed in [31]: The three training runs for model A and model B yield in total 9 combination. By bootstrapping the score difference as described above, we can assess the statistical significance of the score difference between pairs of models individually. Now we set a threshold, relating to the willingness to accept fluctuations due to the randomness of the training process, and declare architecture A superior to architecture B if the fraction of pairwise tests with significant outcomes exceeds the predetermined threshold. As in [31], we use a threshold of 60%.

Test set performance on SEDF The results of our experiments are summarized in Tab. V. As a general observation, either of the two proposed S4Sleep methods represent best-performing methods in the single-channel and multi-channel categories. However surprisingly, the time series-based *S4Sleep(TS)* performs best in the single-channel case and the spectrogram-based *S4Sleep(Spec)* performs best in the multi-channel case. As an interesting observation, *S4Sleep(Spec)* does not show a competitive score in the single-channel case. This effect persists over multiple runs, which is most likely related to peculiarities of the corresponding train and test folds. Even though *S4Sleep(TS)* achieves a nominally higher score than L-SeqSleepNet [25] across multiple runs (assessed as systematic uncertainty), the fact that the latter result is contained within the statistical error bars of the former result, make it seem rather unlikely that the improvement in performance is statistically significant, whereas the difference to SeqSleepNet as the second-best literature result is, under the assumption that the statistical error bars for SeqSleepNet are

of comparable size as those from *S4Sleep(TS)*, statistically significant. The same applies to *S4Sleep(Spec)* in comparison to *XSleepNet1* in the multi-channel setting. We can therefore only claim that *S4Sleep(TS)* is competitive with the current state-of-the-art and both *S4Sleep(TS)* and *S4Sleep(Spec)* are competitive in the multi-channel case. We interpret the inability to discriminate between different algorithms as a hint towards the inadequacy of SEDF as comprehensive benchmarking dataset, mainly due to its limited size.

Performance on SHHS First of all, it is noticeable from the SHHS results in Tab. V that again the proposed S4Sleep models outperform the current state-of-the-art performance both in the single-channel as well as in the multi-channel setting. In this case this even holds for both input representations, i.e., for both for *S4Sleep(TS)* and *S4Sleep(Spec)*. In contrast to the majority of literature approaches, we provide statistical and systematic uncertainty estimates. Both are on the order of 0.001 and therefore comparably small, which underlines the robustness of our results. Unfortunately, no error estimates for the literature results are available. However, under the assumption that the literature results are subject to comparable statistical error estimates as the proposed approaches, *S4Sleep(TS)* would not overlap with the *L-SeqSleepNet*-performance, which would represent a significant improvement in performance. In the multi-channel case the performance difference between the best-performing *S4Sleep(Spec)* with a macro- F_1 score of 0.832 in comparison to the score of *XSleepNet1* with a macro F_1 score 0.823 and, again under the assumption of comparable statistical uncertainties of the literature results, clearly significant. At this point one has to bear in mind that there is presently no generally agreed train-test split available on SHHS, a shortcoming that we aim to address by providing train-test splits as part of the code repository [16] accompanying this submission. On the one hand, this means that scores are strictly speaking not directly comparable. On the other hand, SHHS is already a large-scale dataset, where score fluctuations due to the size of the test set are not expected to play a major role. This is argument is supported by the comparably small statistical uncertainties demonstrated in our analysis. As a final remark, it is worth stressing

TABLE V: Performance of selected models on SEDF and SHHS (test set scores). Notation as in Tab. III.

data set	model	channel	F_1 (\uparrow)					acc. (\uparrow)	macro AUC (\uparrow)	
			macro	W	N1	N2	N3			REM
SEDF	S4Sleep(TS)^{d,o}	single	0.796±0.004±0.004	0.925	0.503	0.854	0.839	0.855	0.839	0.958
	S4Sleep(Spec) ^{d,o}	single	0.777±0.004±0.003	0.918	0.505	0.837	0.791	0.834	0.824	0.962
	L-SeqSleepNet ^{b,n} [25]	single	0.793±0.004	0.916	0.453	0.885	0.862	0.852	0.863	-
	SeqSleepNet ^{b,n} [10]	single	0.786±0.002	0.912	0.447	0.880	0.862	0.830	0.856	-
	SleepTransformer ^{c,1} [32]	single	0.743	0.917	0.404	0.843	0.779	0.772	0.814	-
	IITNet ^{a,m} [33]	single	0.776	0.877	0.434	0.898	0.848	0.824	0.820	-
	S4Sleep(TS) ^{d,n}	multi	0.804±0.002±0.003	0.925	0.568	0.847	0.826	0.863	0.841	0.961
	S4Sleep(Spec)^{d,n}	multi	0.808±0.004±0.002	0.930	0.573	0.848	0.819	0.866	0.843	0.962
	XSleepNet1 ^{b,1} [34]	multi	0.806	0.922	0.518	0.880	0.868	0.839	0.863	-
	XSleepNet2 ^{b,1} [34]	multi	0.800	0.913	0.495	0.880	0.869	0.842	0.860	-
	RobustSleepNet ^{d,j} [30]	multi	0.778	-	-	-	-	-	-	-
	U-Sleep ^{e,q} [7]	multi	0.79	0.93	0.57	0.86	0.71	0.88	-	-
SalientSleepNet ^{c,1} [35]	multi	0.795	0.933	0.542	0.858	0.783	0.858	0.841	-	
SHHS	S4Sleep(TS)^{f,p}	single	0.817±0.001±0.001	0.931	0.526	0.888	0.848	0.895	0.882	0.977
	S4Sleep(Spec) ^{f,p}	single	0.815±0.001±0.0005	0.931	0.505	0.884	0.853	0.931	0.882	0.977
	L-SeqSleepNet ^{f,p} [25]	single	0.814	0.931	0.511	0.890	0.849	0.898	0.884	-
	SeqSleepNet ^{f,p} [10]	single	0.802	0.918	0.491	0.882	0.835	0.882	0.872	-
	SleepTransformer ^{f,p} [32]	single	0.801	0.922	0.461	0.883	0.852	0.886	0.877	-
	XSleepNet1 ^{f,p} [25]	single	0.807	0.916	0.514	0.885	0.850	0.884	0.876	-
	XSleepNet2 ^{f,p} [25]	single	0.810	0.920	0.499	0.883	0.850	0.882	0.875	-
	IITNet ^{f,o} [33]	single	0.798	0.901	0.481	0.884	0.852	0.872	0.867	-
	S4Sleep(TS) ^{f,p}	multi	0.827±0.001±0.002	0.938	0.536	0.894	0.849	0.919	0.890	0.980
	S4Sleep(Spec)^{f,p}	multi	0.832±0.0005±0.0001	0.942	0.539	0.898	0.856	0.919	0.895	0.981
	XSleepNet1 ^{f,p} [34]	multi	0.823	-	-	-	-	-	0.891	-
	XSleepNet2 ^{f,p} [34]	multi	0.822	-	-	-	-	-	0.891	-
RobustSleepNet ^{g,i} [30]	multi	0.792	-	-	-	-	-	-	-	
U-Sleep ^{e,r} [7]	multi	0.80	0.93	0.51	0.87	0.76	0.92	-	-	

a: based on SEDF-SC (20 recordings) b: based on SEDF-SC (39 recordings) c: based on SEDF-SC (153 recordings) d: based on full SEDF (197 recordings) e: trained on recordings from various datasets. f: based on SHHS visit 1. g: based on SHHS visit 2. h: based on full SHHS. i: 3-fold crossvalidation. j: 5-fold crossvalidation. k: 10-fold crossvalidation. l: 20-fold crossvalidation. m: leave-one-subject-out crossvalidation. n: 8:1:1 training-validation-test holdout set evaluation. o: 5:2:3 training-validation-test holdout set evaluation. p: 7:3 training-test holdout set evaluation. q: test on sampled recordings from SEDF-SC. r: test on sampled recordings from full SHHS.

that the exceptionally strong performance of both *S4Sleep*-variants without further hyperparameter adjustments is a very good sign for the generalization capabilities of the proposed architecture, which will therefore be interesting to explore on other datasets and even in entirely different data modalities.

General remarks First, it is worth stressing that the proposed models were optimized towards an optimal macro F_1 -score by means of model selection on the validation set. Therefore other observables reported in Tab. V should just be seen as supplementary information for the reader but could be further improved by specifically optimizing towards them. Second, the two *S4Sleep*-variants show the same ranking on SHHS as in the case of the SEDF dataset, namely *S4Sleep(TS)* dominates in the single-channel case and *S4Sleep(Spec)* in the multi-channel case. More specifically, on SHHS the differences between both models turn out to be significant in the sense put forward at the beginning of this section. It remains an interesting open question if improved model architectures would allow to train competitive time-series-based models in the multi-channel case. Third, we also use the established

methodology to also assess the statistical significance of using multiple instead of a single epoch as input. To this end, for given channel configuration and input modality, we compare the best-performing single-epoch model as identified by Tab. II and the best-performing multi-epoch model as identified by Tab. III. In all cases, we were able to demonstrate significant performance differences between single- and multi-epoch models at a predefined threshold of 60% of pairwise tests following the methodology introduced above. These results reiterate the empirical findings of [10] and emphasize the significant advantage of jointly predicting multiple sleep stages for multiple input epochs at once, which allows to leverage more contextual information into each single-epoch prediction.

Finally, it is worth pointing out that *S4Sleep(TS)* is the first approach that demonstrates the competitiveness of raw time series as sole input representation for sleep staging. In particular, *S4Sleep(TS)* achieved a score that is competitive or even superior to L-SeqSleepNet both on SHHS and SEDF without explicitly leveraging long-range correlations across hundreds of sleep epochs [25], which the authors identify

as central aspect for the performance improvement over prior state-of-the-art. Again, it remains to see whether for example a careful gradual up-scaling of the input size during the training procedure eventually to 200 epochs could lead to a further improvement of the model performance, in particular in the case of *S4Sleep(TS)*.

IV. SUMMARY AND OUTLOOK

Summary In this work, we addressed the problem of automatic sleep staging from polysomnography, which represents a time series classification task where sleep stages have to be predicted per epoch comprising 30 seconds. Starting with models operating on a single epoch as input, we systematically searched for the most appropriate model architectures within an encoder-predictor modeling paradigm. Both for raw time series as well as for spectrograms as input, we identify the recently proposed structured state space models as best predictor architecture. Extending the input size to multiple epochs as input, we find hints for the superiority of epoch encoders to summarize epochs or sub-epochs into a temporally downsampled representation that is then subsequently processed with appropriate predictor models. In this way, we identify optimal model architectures, *S4Sleep(TS)* and *S4Sleep(Spec)*, both for raw time series and spectrograms as input representations. These model turn out to be competitive with the existing state-of-the-art on the smaller SEDF dataset and outperform the current state-of-the-art on the large-scale SHHS dataset both in the case of single-channel as well as multi-channel input. In particular, *S4Sleep(TS)* represents one of the rare cases of competitive model performance of a raw-time-series-based model compared to the dominating paradigm of spectrogram-based methods in the field. The code underlying our experiments is publicly available [16].

Outlook We take the fact that both model variants show a very strong performance on SHHS both in the single- and multi-channel input representations without any further hyperparameter adjustments as a sign for the generalization capabilities of the proposed model architectures. We therefore consider it as a very promising step to also explore these models in the context of other data modalities with physiological time series, such as long-term ECG classification, clinical EEG or PPG classification or regression, or even to time series classification task beyond physiological time series such as audio classification. In any case, the present work presents a blueprint for a structured assessment of optimal model architectures also in other domains. As briefly discussed in the previous section, there are several directions to further enhance the model performance, ranging from leveraging interactions across very long input sequences, improved architectures for handling multi-channel input and finally more elaborate pre-training schemes.

ACKNOWLEDGMENT

The authors thank Insa Wolf and Fabian Radtke for discussions.

REFERENCES

- [1] L. A. Panossian and A. Y. Avidan, "Review of sleep disorders," *Medical Clinics of North America*, vol. 93, no. 2, pp. 407–425, 2009.
- [2] M. K. Pavlova and V. Latreille, "Sleep disorders," *The American journal of medicine*, vol. 132, no. 3, pp. 292–299, 2019.
- [3] C. Iber, S. Ancoli-Israel, A. L. Chesson, S. F. Quan *et al.*, *The AASM manual for the scoring of sleep and associated events: rules, terminology and technical specifications*. American academy of sleep medicine Westchester, IL, 2007, vol. 1.
- [4] J. A. Hobson, "A manual of standardized terminology, techniques and scoring system for sleep stages of human subjects," *Electroencephalography and clinical neurophysiology*, vol. 26, no. 6, p. 644, 1969.
- [5] H. Danker-Hopfe, P. Anderer, J. Zeithofer, M. Boeck, H. Dorn, G. Gruber *et al.*, "Interrater reliability for sleep scoring according to the Rechtschaffen & Kales and the new AASM standard," *Journal of Sleep Research*, vol. 18, no. 1, pp. 74–84, Mar. 2009.
- [6] R. S. Rosenberg and S. V. Hout, "The American academy of sleep medicine inter-scoring reliability program: Sleep stage scoring," *Journal of Clinical Sleep Medicine*, vol. 09, no. 01, pp. 81–87, Jan. 2013.
- [7] M. Perslev, S. Darkner, L. Kempfner, M. Nikolic, P. J. Jennum, and C. Igel, "U-sleep: resilient high-frequency sleep staging," *npj Digital Medicine*, vol. 4, no. 1, Apr. 2021.
- [8] H. Phan, O. Y. Chen, M. C. Tran, P. Koch, A. Mertins, and M. D. Vos, "XSleepNet: Multi-view sequential model for automatic sleep staging," *IEEE Transactions on Pattern Analysis and Machine Intelligence*, pp. 1–1, 2021.
- [9] G. Brandmayr, M. Hartmann, F. Fürbass, and G. Dorffner, "Self-attention long-term dependency modelling in electroencephalography sleep stage prediction," in *Neural Information Processing*. Springer International Publishing, 2021, pp. 379–390.
- [10] H. Phan, F. Andreotti, N. Cooray, O. Y. Chén, and M. De Vos, "Seqsleepnet: end-to-end hierarchical recurrent neural network for sequence-to-sequence automatic sleep staging," *IEEE Transactions on Neural Systems and Rehabilitation Engineering*, vol. 27, no. 3, pp. 400–410, 2019.
- [11] A. Gu, K. Goel, and C. Ré, "Efficiently modeling long sequences with structured state spaces," in *International Conference on Learning Representations*, 2022.
- [12] T. Mehari and N. Strodthoff, "Towards quantitative precision for ECG analysis: Leveraging state space models, self-supervision and patient metadata," *IEEE Journal of Biomedical and Health Informatics*, pp. 1–9, 2023.
- [13] M. M. Bronstein, J. Bruna, T. Cohen, and P. Veličković, "Geometric deep learning: Grids, groups, graphs, geodesics, and gauges," *arXiv preprint 2104.13478*, 2021.
- [14] J. Schmidhuber, "Learning complex, extended sequences using the principle of history compression," *Neural Computation*, vol. 4, no. 2, pp. 234–242, 1992.
- [15] Y. LeCun, "A path towards autonomous machine intelligence version 0.9. 2, 2022-06-27," *Open Review*, vol. 62, 2022.
- [16] T. Wang and N. Strodthoff, "Source code for: S4Sleep: Elucidating the design space of deep-learning-based long time series classification models- a case study based on sleep staging, version 1.0," *Zenodo*. <https://doi.org/10.5281/xxxx>, Oct. 2023.
- [17] A. Radford, J. W. Kim, T. Xu, G. Brockman, C. McLeavey, and I. Sutskever, "Robust speech recognition via large-scale weak supervision," in *International Conference on Machine Learning*. PMLR, 2023, pp. 28 492–28 518.
- [18] S. Hochreiter and J. Schmidhuber, "Long short-term memory," *Neural computation*, vol. 9, no. 8, pp. 1735–1780, 1997.
- [19] A. Vaswani, N. Shazeer, N. Parmar, J. Uszkoreit, L. Jones, A. N. Gomez *et al.*, "Attention is all you need," *Advances in neural information processing systems*, vol. 30, 2017.
- [20] A. Baeovski, Y. Zhou, A. Mohamed, and M. Auli, "wav2vec 2.0: A framework for self-supervised learning of speech representations," *Advances in neural information processing systems*, vol. 33, pp. 12 449–12 460, 2020.
- [21] B. Kemp, A. H. Zwinderman, B. Tuk, H. A. Kamphuisen, and J. J. Obery, "Analysis of a sleep-dependent neuronal feedback loop: the slow-wave microcontinuity of the eeg," *IEEE Transactions on Biomedical Engineering*, vol. 47, no. 9, pp. 1185–1194, 2000.
- [22] A. L. Goldberger, L. A. Amaral, L. Glass, J. M. Hausdorff, P. C. Ivanov, R. G. Mark *et al.*, "Physiobank, physiotoolkit, and physionet: components of a new research resource for complex physiologic signals," *circulation*, vol. 101, no. 23, pp. e215–e220, 2000.

- [23] D.-M. Ross and E. Cretu, "Probabilistic modelling of sleep stage and apneic events in the university college of dublin database (ucddb)," in *2019 IEEE 10th Annual Information Technology, Electronics and Mobile Communication Conference (IEMCON)*. IEEE, 2019, pp. 0133–0139.
- [24] S. F. Quan, B. V. Howard, C. Iber, J. P. Kiley, F. J. Nieto, G. T. O'Connor *et al.*, "The sleep heart health study: design, rationale, and methods," *Sleep*, vol. 20, no. 12, pp. 1077–1085, 1997.
- [25] H. Phan, K. P. Lorenzen, E. Heremans, O. Y. Chén, M. C. Tran, P. Koch *et al.*, "L-SeqSleepNet: Whole-cycle long sequence modelling for automatic sleep staging," *IEEE Journal of Biomedical and Health Informatics*, pp. 1–10, 2023.
- [26] T.-Y. Lin, P. Goyal, R. Girshick, K. He, and P. Dollár, "Focal loss for dense object detection," in *Proceedings of the IEEE international conference on computer vision*, 2017, pp. 2980–2988.
- [27] L. N. Smith, "Cyclical learning rates for training neural networks," in *2017 IEEE winter conference on applications of computer vision (WACV)*. IEEE, 2017, pp. 464–472.
- [28] I. Loshchilov and F. Hutter, "Decoupled weight decay regularization," in *International Conference on Learning Representations*, 2018.
- [29] S. Bates, T. Hastie, and R. Tibshirani, "Cross-validation: What does it estimate and how well does it do it?" *Journal of the American Statistical Association*, pp. 1–12, May 2023.
- [30] A. Guillot and V. Thorey, "Robustsleepnet: Transfer learning for automated sleep staging at scale," *IEEE Transactions on Neural Systems and Rehabilitation Engineering*, vol. 29, pp. 1441–1451, 2021.
- [31] T. Mehari and N. Strodthoff, "Self-supervised representation learning from 12-lead ECG data," *Computers in Biology and Medicine*, vol. 141, p. 105114, Feb. 2022.
- [32] H. Phan, K. Mikkelsen, O. Y. Chén, P. Koch, A. Mertins, and M. De Vos, "Sleeptransformer: Automatic sleep staging with interpretability and uncertainty quantification," *IEEE Transactions on Biomedical Engineering*, vol. 69, no. 8, pp. 2456–2467, 2022.
- [33] H. Seo, S. Back, S. Lee, D. Park, T. Kim, and K. Lee, "Intra-and inter-epoch temporal context network (iitnet) using sub-epoch features for automatic sleep scoring on raw single-channel eeg," *Biomedical signal processing and control*, vol. 61, p. 102037, 2020.
- [34] H. Phan, O. Y. Chén, M. C. Tran, P. Koch, A. Mertins, and M. De Vos, "Xsleepnet: Multi-view sequential model for automatic sleep staging," *IEEE Transactions on Pattern Analysis and Machine Intelligence*, vol. 44, no. 9, pp. 5903–5915, 2021.
- [35] Z. Jia, Y. Lin, J. Wang, X. Wang, P. Xie, and Y. Zhang, "Salientsleepnet: Multimodal salient wave detection network for sleep staging," *arXiv preprint arXiv:2105.13864*, 2021.

APPENDIX A

ADDITIONAL RESULTS

Tab. VI shows the performance of the best-performing single-epoch models from Tab. II trained and evaluated on the SEDF dataset (test set scores). These results provide quantitative insights on the performance gains achieved through predicting several epochs at once.

TABLE VI: Performance of selected models using a single epoch as input on SEDF. Notation as in Tab. III.

model	channel	F_1 (\uparrow)						acc. (\uparrow)	macro AUC (\uparrow)
		macro	W	N1	N2	N3	REM		
CNN+S4(TS)	single	0.752±0.003±0.002	0.903	0.415	0.850	0.822	0.770	0.807	0.948
None+S4(Spec)	single	0.730±0.007±0.004	0.890	0.382	0.834	0.782	0.760	0.793	0.937
CNN+S4(TS)	multi	0.769±0.002±0.004	0.908	0.488	0.840	0.812	0.796	0.814	0.952
None+S4(Spec)	multi	0.780±0.002±0.003	0.926	0.487	0.840	0.829	0.817	0.826	0.955